# Environmental, Biochemical, and Genetic Drivers of DMSP Degradation and DMS Production in the Sargasso Sea

Naomi Marcil Levine[1]
Vanessa A. Varaljay[2]
Dierdre A. Toole[3]
John W.H. Dacey[4]
Scott C. Doney[3]
Mary Ann Moran[5]

[1] MIT-WHOI Joint Program, Woods Hole, MA 02543
now at: OEB Department, Harvard University, Cambridge MA 02138

[2] Department of Microbiology, University of Georgia, Athens GA 30602

[3] Marine Chemistry and Geochemistry, Woods Hole Oceanographic Institution, Woods Hole, MA 02543

[4] Biology, Woods Hole Oceanographic Institution, Woods Hole, MA 02543

[5] Department of Marine Sciences, University of Georgia, Athens GA 30602

Running head: Drivers of DMSP degradation and DMS production

Corresponding author:
Naomi Marcil Levine,
nlevine@oeb.harvard.edu
OEB Department, Harvard University, Cambridge MA 02138

This is the pre-peer reviewed version of the following article:

**Levine, N. M., Varaljay, V. A., Toole, D. A., Dacey, J. W. H., Doney, S. C. and Moran, M. A. (2012), Environmental, biochemical and genetic drivers of DMSP degradation and DMS production in the Sargasso Sea. Environmental Microbiology. doi: 10.1111/j.1462-2920.2012.02700.x**

which has been published in final form at http://onlinelibrary.wiley.com/doi/10.1111/j.1462-2920.2012.02700.x/abstract

**Summary**

Dimethylsulfide (DMS) is a climatically relevant trace gas produced and cycled by the surface ocean food web. Mechanisms driving intraannual variability in DMS production and dimethylsulfoniopropionate (DMSP) degradation in open-ocean, oligotrophic regions were investigated during a 10 month time-series at the Bermuda Atlantic Time-series Study site in the Sargasso Sea. Abundance and transcription of bacterial DMSP degradation genes, DMSP lyase enzyme activity, and DMS and DMSP concentrations, consumption rates, and production rates were quantified over time and depth. This interdisciplinary dataset was used to test current hypotheses of the role of light and carbon supply in regulating upper-ocean sulfur cycling. Findings supported UV-A dependent phytoplankton DMS production. Bacterial DMSP-degraders may also contribute significantly to DMS production when temperatures are elevated and UV-A dose is moderate, but may favor DMSP demethylation under low UV-A doses. Three groups of bacterial DMSP degraders with distinct intraannual variability were identified and niche differentiation was indicated. The combination of genetic and biochemical data suggest a modified 'bacterial switch' hypothesis where the prevalence of different bacterial DMSP degradation pathways is regulated by a complex set of factors including carbon supply, temperature, and UV-A dose.

## INTRODUCTION

Dimethylsulfide (DMS) is produced and cycled in marine ecosystems by the surface ocean food web and is the predominant source of natural sulfur to the atmosphere. Once ventilated to the atmosphere, DMS is oxidized to sulfate and methane sulfonate aerosols (Shaw, 1983), which act as cloud condensation nuclei. Perturbations in DMS ventilation rates have the potential to alter aerosol abundance, cloud coverage, and cloud properties, which in turn affect the atmospheric radiative balance and Earth's climate (Charlson et al., 1987). Changes in marine physical and chemical properties, such as those projected to occur under high atmospheric $CO_2$ conditions, have the potential to affect DMS production by altering community composition, rates of primary production, and heterotrophic microbial activity. An improved understanding of the mechanisms driving DMS production is needed before accurate predictions of the response of the marine sulfur cycle to anthropogenically induced changes can be made.

The primary precursor of DMS, dimethylsulfoniopropionate (DMSP), is produced in surface waters by marine phytoplankton. While phytoplankton directly convert some DMSP to DMS, the majority of the intracellular DMSP pool (particulate DMSP, DMSPp) is released as DMSP into the water column (Simó et al., 2002). This dissolved pool of DMSP (DMSPd) is then rapidly cycled by marine bacterioplankton that degrade DMSP via two competing, enzymatically mediated, pathways (Cantoni and Anderson, 1956; Taylor and Gilchrist, 1991; Kiene et al., 2000). The DMSP demethylation pathway provides bacteria with both carbon and reduced sulfur compounds that are easily incorporated into amino acids and cellular biomass (Kiene, 1996; Kiene and Linn, 2000; Kiene et al., 2000). The DMSP cleavage pathway yields an easily accessible 3-carbon compound (acrylate or 3-hydroxy propionate) and the volatile DMS molecule. Phytoplankton and bacterial DMSP cleavage are the only known pathways that result

in the release of DMS into the water column. Due to bacterial DMSP demethylation and DMS consumption processes, only a small percentage (1-2%) of DMSP produced by marine phytoplankton is ventilated to the atmosphere as DMS (Bates et al., 1994; Kwint and Kramer, 1996). Therefore, understanding the conditions under which DMSP cleavage is favorable relative to demethylation is essential for quantifying current DMS emissions and predicting future emissions.

Light has been hypothesized to play an important role in upper ocean sulfur cycling (Toole and Siegel, 2004; Vallina and Simó, 2007). Previous work suggests that phytoplankton cleave DMSP to DMS as an anti-oxidant response to UV radiation (Sunda et al., 2002) and that UV radiation inhibits bacterial DMSPd and DMS consumption rates (Slezak et al., 2007). On the other hand, Kiene *et al*. (2000) and Simó (2001) hypothesize that the regulation between the two competing bacterial transformations of DMSP (the 'bacterial switch') is driven by bacterial carbon and sulfur demands and by DMSP availability. These authors postulate that the demethylation pathway will be favorable when DMSPd supply is low relative to bacterial carbon and sulfur demands, and cleavage will be favored under low bacterial sulfur demand and elevated DMSPd supply.

The ability to demethylate DMSP is widespread in the marine bacterioplankton community. Homologs of the gene responsible for the demethylation of DMSP (*dmdA*) are harbored by up to 58% of bacterioplankton cells sampled in the Global Ocean Sampling (GOS) metagenome and at least 80% of *Roseobacter* cells and 40% of SAR11 cells sampled in the Sargasso Sea metagenome (Howard et al., 2006; Howard et al., 2008). These metagenomic analyses support Micro-FISH studies and enrichment experiments that show SAR11 and *Roseobacter* clades as major players in DMSP cycling in the Sargasso Sea (Ledyard et al., 1993;

Malmstrom et al., 2004b; Malmstrom et al., 2004a). The *dmdA* gene can be grouped into 5 protein clades and further into 14 subclades based on nucleotide diversity (Howard et al., 2008; Varaljay et al., 2010). In this study, we focus on the three most abundant *dmdA* clades in the Sargasso Sea: clades A (*Roseobacter*), C (SAR11), and D (SAR11). Several bacterial DMS-producing genes have also recently been identified; *dddD, dddL, dddP*, *dddQ*, *dddW*, and *dddY* (Todd et al., 2007; Curson et al., 2008; Todd et al., 2009; Curson et al., 2011; Todd et al., 2011; Todd et al., 2012). We focus on *dddP* (*Roseobacter*) as metagenomic data and preliminary studies indicate that this gene, along with *dddQ*, is an order of magnitude more abundant than *dddD*, *dddL, dddW* and *dddY* in the Sargasso Sea (Todd et al., 2009; this study).

We investigate intraannual variability and the role of light and carbon availability on microbial and phytoplankton DMS and DMSP (DMS(P)) cycling in an open-ocean, low nutrient, oligotrophic region. During a 10 month study at the Bermuda Atlantic Time-series Study (BATS) station, we quantified the abundance and transcription of key genes involved in the competing DMSP degradation pathways (*dmdA*, *dddP*) and the potential activity of the enzymes involved in bacterial and phytoplankton DMS production. This interdisciplinary dataset provides insight into the activity, diversity, and variability of key genomic groups responsible for organic sulfur cycling that would not be possible with chemical or biological measurements alone.

## RESULTS

### Seasonality in DMS(P) concentrations

A strong seasonal DMS(P) cycle is observed at BATS. Upper ocean (< 80 m) DMSPp concentrations typically peak in the spring concurrent with the shoaling of the mixed layer and remain high throughout the summer until fall mixing events. Mixed layer DMS concentrations

(Fig. 1) peak several months after DMSPp concentrations (Dacey et al., 1998; this study). In 2008, upper ocean DMSPd consumption rates were highest during the summer and early fall and were positively correlated both with DMSPd concentrations ($r^2$=0.54, $p<0.01$) (Fig. 2e) and with mixed layer DMSPd loss rate constants ($r^2$=0.35, $p<0.01$). DMS consumption was elevated in the mixed layer throughout the year and in the subsurface (20 - 60 m) in the early summer (Fig. 2f).

The typical seasonal cycle was perturbed in 2008 by a series of events that provided an opportunity to test hypotheses about mechanisms driving upper-ocean sulfur cycling. In May, BATS was under the influence of a mature or decaying cyclonic eddy (D. McGillicuddy, *personal comm.*). The presence of this upwelling eddy coincided with elevated subsurface DMSP concentrations and DMS(P) consumption rates (Fig. 2b,c,e,f). The BATS site was also heavily influenced by Hurricane Bertha for 4 days immediately preceding the July cruise. Surface waters rapidly restratified, but the remnant of the deep mixing event was still evident during the July sampling, including lower DMS(P) concentrations relative to typical mid-summer values (Fig. 1 & 2b,c). Increased vertical mixing, increased ventilation of DMS to the atmosphere, and low UV radiative dose from greater convection and cloud cover may have directly or indirectly (through phytoplankton DMSPp production) affected DMS(P) cycling in July.

**Abundance of Bacterial DMSP Degradation Genes**

Variability in the abundance of the DMSP demethylation gene (*dmdA* subclades A/1, A/2, C/2, D/1, and D/3) and the DMSP cleavage gene (*dddP*) over the 10 month time-series was quantified using the quantitative polymerase chain reaction (qPCR) (Fig. 3). The abundance and

112 seasonal variations of *dmdA* and *dddP* in 2008 were consistent with that of the heterotrophic
113 microbial community that has been described previously for this site (e.g. Carlson et al., 2009;
114 Vila-Costa et al., 2010). *dmdA* subclade D/1 (SAR11) was the most abundant subclade with an
115 average of $4.6x10^7$ copies per liter seawater and a maximum of $1.4x10^8$ copies per liter (May 60
116 m). The abundances of the other *dmdA* subclades quantified during this study were significantly
117 lower than D/1 with average copies per liter seawater ranging from $1.4x10^5$ (A/2, *Roseobacter*)
118 to $5.5x10^6$ (C/2, SAR11). *dddP* (*Roseobacter*) was the second most abundant DMSP degradation
119 gene with an average abundance of $1.2x10^7$ copies per liter seawater and a maximum of $5.0x10^7$
120 copies per liter (May 60 m). We estimate that up to 33% of sampled bacterioplankton cells
121 contained a copy of *dmdA* and up to 11% of cells contained a copy of *dddP*, based on total
122 bacterial cell counts as per Howard *et al.* (2008). Significant variability in the total abundance of
123 DMSP degradation genes was observed, with the highest abundances seen during the summer at
124 depth and the lowest abundances seen during the winter and in surface waters.
125 DMSP gene abundance data separated into three groups with distinct intraannual
126 variability (*Supplementary material S1*): Group I contained *dddP* and *dmdA* subclades A/1 and
127 D/3 which were correlated with an $r^2>0.65$ ($p<0.01$); Group II contained *dmdA* subclades A/2
128 and D/1 which were correlated with an $r^2=0.63$ ($p<0.01$); and Group III contained *dmdA*
129 subclade C/2 which was not correlated with *dmdA* A/1 or *dddP* ($r^2<0.03$, $p>0.30$) and was
130 weakly correlated with *dmdA* A/2, D/1, and D/3 ($r^2<0.31$, $p<0.01$). The distinct temporal and
131 depth patterns exhibited by the three DMSP gene groups suggest that they were responding to
132 different chemical and physical forcings. A strong correlation between *dddP* and *dmdA* subclade
133 A/1 (both *Roseobacter*) gene copy number was observed ($r^2 = 0.89$, $p <0.01$), although the gene
134 stoichiometry (*dddP*:A/1) was ~30:1. *dmdA* subclade C/2, believed to be harbored by SAR11

bacteria, was spatially and temporally distinct from *dmdA* clades D/1 (also SAR11) and A/1 (*Roseobacter*). The seasonal succession of C/2, with peak abundance occurring 5-6 months after the winter mixing event, coincides with seasonal variations observed at BATS for the SAR11 subclade Ia (Carlson et al., 2009).

**Transcription of Bacterial DMSP Degradation Genes**

Over the 10 month sampling period, DMSP degradation genes (*dddP* and *dmdA* subclades A/1, D/1, and D/3) all showed similar low levels of transcription, with less than 1 transcript per 1000 gene copies based on qPCR estimates. *dmdA* D/1 had the highest measured transcription with a maximum of $3.8 \times 10^4$ copies per liter seawater (Oct 60 m) and an average of 1 transcript per 5000 copies. This low level of transcription is consistent with previous metatranscriptomic data from the Sargasso Sea, Sapelo Island, and North Pacific Subtropical Gyre and with qPCR studies in the North Pacific Subtropical Gyre and Monterey Bay (Vila-Costa et al., 2010; Gifford et al., 2011; Varaljay et al., submitted; Varaljay et al. unpublished data). Significant temporal and depth variations in gene transcription were nonetheless detected.

The highest transcript numbers for both *dmdA* and *dddP* were observed at 40 – 60 m during the summer and early fall, and throughout the water column in February 2008 (Fig. 4). With few exceptions (most notably February), all samples with significant DMSP gene transcription also showed elevated rates of DMSPd consumption (Fig. 2e & 4), where 'elevated' is defined as > 1σ above the mean. However, 41% of samples without significant DMSP gene transcription levels nonetheless had elevated DMSPd consumption rates, specifically surface waters throughout the summer, and upper water column (< 40 m) samples in May, August and September. Due to practical limitations of nucleic acid quantities, the transcription analysis

158 focused on *dddP* and three *dmdA* subclades (A/1, D/1, and D/3) chosen based on metagenomic
159 data, preliminary studies, and a significant positive correlation between measured abundance and
160 DMSPd consumption rates ($p<0.02$). However, a different *dmdA* subclade or DMSP cleavage
161 gene that was not targeted in qPCR (e.g. *dmdA* subclades C/2, A/2, B/3, or E/3 or cleavage genes
162 *dddD*, *dddL*, *dddQ*, *dddY* and *dddW*) may have been responsible for the DMSPd consumption in
163 water masses without detectable *dmdA* A/1, D/1, D/3, or *dddP* transcription. In February,
164 elevated *dmdA* transcription at most depths and for most subclades (Fig. 4) suggested that the
165 bacterial community was actively consuming DMSP, yet the DMSPd consumption rate was not
166 significantly elevated. The driving mechanisms behind higher *dmdA* transcription in this month
167 are unclear.

168 Transcription of *dmdA* subclade D/1, the subclade with the highest gene copy and
169 transcript numbers, was significantly negatively correlated with UV-A dose (Table 1). In
170 addition, all significant D/1 transcription with the exception of the October 40 m sample
171 occurred at a UV-A dose less than 20% of the average summer surface incident UV-A (Table 1).
172 Here we focus on UV-A dose as this wavelength correlated best with changes in the sulfur cycle
173 and has been identified by previous studies as an important regulator of DMSP consumption and
174 DMS production (e.g. Slezak et al., 2001; Toole et al., 2003; Slezak et al., 2007). We found a
175 significant positive relationship between D/1 transcript number and DMSPd concentration and a
176 significant negative relationship between D/1 transcript number and total organic carbon (TOC)
177 concentration. This suggests that carbon supply, in particular the relative abundance of DMSPd
178 compared to TOC, may play a role in the transcription of the most abundant *dmdA* subclade. A
179 significant relationship between D/1 transcript number and bacterial carbon demand or total
180 bacterial cell counts was not observed. Finally, a significant negative relationship between D/1

transcript number and DMS concentration was seen, suggesting that conditions favorable for DMS production may be unfavorable for DMSP demethylation by bacteria that harbor this *dmdA* subclade.

**DMS production: potential enzyme activity**

The potential DMSP lyase assay has been used previously as a proxy for the activity of the phytoplankton DMSP lyase pathway and for potential phytoplankton DMS production (Steinke et al., 2002; Harada et al., 2004; Bell et al., 2007). Here we quantified both phytoplankton and bacterial DMSP lyase activity (DLA) to provide insight into DMS production at BATS. These two pools are operationally defined based on size as per convention where the bacterial fraction was 0.2 – 1.2 μm and the phytoplankton fraction was > 1.2μm. Therefore, phytoplankton smaller than 1.2 μm were included in the bacterial fraction whereas phytoplankton-associated bacteria were included in the phytoplankton fraction. The dominant picophytoplankton, *Prochlorococcus* and *Synechococcus*, produce negligible amounts of DMS (Keller et al., 1989) so are not believed to have contributed significantly to the measured bacterial DLA. Here we focus on differences in temporal and spatial patterns in bacterial and phytoplankton DLA over the sampling period as the rates measured for these two groups are not directly comparable. Phytoplankton DLAs were measured on cell extracts and are presented as specific rates whereas bacterial DLAs were measured on whole cells and are presented as absolute rates. In addition, different DMSP cleavage enzymes in phytoplankton versus bacteria may have performed differently in the DLA assay.

Phytoplankton DLA was highest in surface waters in the spring, summer, and early fall (Fig. 5a) concurrent with the shoaling of the mixed layer and was positively correlated with UV-A radiation dose (Table 1). In addition, 88% of elevated phytoplankton enzyme activity, defined

as >1σ above the mean, occurred under moderate to high light conditions, defined as UV-A dose greater than 20% of the average summer surface incident UV-A (Table 1). Phytoplankton DLA was also significantly correlated with TOC, DMS concentration, and temperature (Table 1), variables that were also significantly correlated with one another ($r^2$>0.42, p<0.01) and displayed strong seasonality. Only 11% (r = 0.33) of the variability in phytoplankton DLA could be explained by DMSPp concentrations (Table 1) and there was no significant relationship between phytoplankton DLA and Chlorophyll a (not shown), indicating that DMSPp concentration and Chlorophyll a alone may not be good proxies for phytoplankton DMS production at BATS. Variation in eukaryotic phytoplankton group pigment concentrations, as identified by high-performance liquid chromatography (HPLC), explained less than 20% of the observed variations in DMSPp concentrations and phytoplankton DLA rates (*Supplemental Material S2)*. This further suggests that physical (e.g. UV stress) and chemical conditions may be equally or more important than taxonomic identity in determining DMSPp concentrations and phytoplankton DLA rates at BATS.

Potential bacterial DMS production, defined as DLA*DMSPd, was highest in the late summer and early fall between 20 m and 60 m (Fig. 5b). Bacterial DLA and potential DMS production were significantly correlated with month, temperature and DMS concentration (Table 1), suggesting that bacterial DMS production may be a relevant source of DMS at certain times of year. While there was no significant correlation between UV-A dose and bacterial DMS production, 67% of elevated bacterial DLA and 33% of elevated potential bacterial DMS production, defined as >1σ above the mean, occurred under moderate to high light conditions (Table 1). This suggests that bacterial DMS production was UV-A tolerant. A significant positive relationship between bacterial DLA and DMSPd concentration and bacterial DLA and

227 the ratio of DMSPd:TOC was observed (Table 1). However, these variables could only explain
228 8% and 23% of the variability in bacterial DLA, respectively, indicating that carbon availability
229 may not be the primary process regulating bacterial DMS production.

230 Six of the eight samples with measurable *dddP* transcription had measurable bacterial
231 DMSP lyase activity (Fig. 5b). Several samples, however, showed elevated bacterial DLA yet
232 had no *dddP* transcription. This might occur if DMSP cleavage enzymes have long half-lives,
233 such that cells only need to actively transcribe the *dddP* gene intermittently. Alternatively, *dddP*,
234 although most abundant, may not have been the primary bacterial DMSP cleavage gene being
235 expressed at BATS.

236

237 **DISCUSSION**

238 DMSP degradation gene data were integrated with observations of physical and
239 biogeochemical parameters relevant to the seasonal DMS(P) cycle in the Sargasso Sea using a
240 non-metric multidimensional scaling (MDS) framework. The two gene groups defined initially
241 based on correlation analysis (Fig. S1) also emerged in the MDS analysis (Fig. 6). Group I
242 (*dmdA* A/1, *dmdA* D/3, *dddP*) and Group II (*dmdA* A/2, *dmdA* D/1) separated along MDS axis 2,
243 which explained 8% of the total variance and was positively correlated with date ($r=0.66$,
244 $p<0.01$), temperature ($r=0.57$, $p<0.01$), and DMSPd concentrations ($r=0.50$, $p<0.01$). This is
245 consistent with a higher abundance of cells containing Group I subclades in the winter and spring
246 when temperature and DMSPd concentrations were low, and an increased abundance of Group II
247 subclades in the summer and fall when temperature and DMSPd concentrations were elevated.
248 MDS axis 1 (Fig. 6) accounted for 84% of the total variance and correlated best with DMS
249 concentration ($r=0.59$, $p<0.01$), bacterial abundance ($r=-0.49$, $p=0.02$), bacterial carbon demand

(r=-0.47 $p<0.01$) and UV-A dose (r=0.38, p=0.03). We hypothesize that this axis represents depth-dependent niche differentiation among bacteria harboring DMSP degradation genes, potentially driven by radiation dose or carbon availability. The two *Roseobacter dmdA* gene clades (A/1 and A/2) are particularly well separated along this MDS axis and indeed show opposite depth distributions that are especially evident during the summer (Fig. 3c,d).

To explore potential mechanisms driving DMSP cleavage versus DMSP demethylation, a second MDS analysis was conducted using only measures of activity: *dmdA* D/1 transcript numbers, bacterial DLA*DMSPd, and phytoplankton DLA. MDS axis 1, which explained 47% of the total variance, separated DMSP cleavage (potential phytoplankton and bacterial DMS production) from DMSP demethylation (*dmdA* D/1 transcription). This axis was positively correlated with date (r=0.54, $p<0.01$), TOC (r=0.48, $p<0.01$), UV-A dose (r=0.39, p=0.04) and DMS concentration (r=0.37, p=0.02). MDS axis 2, which explained 27% of the total variance and was best correlated with DMSPd concentration and DMSPd:TOC (r=0.48, $p<0.01$ for both), separated bacterial activity (bacterial DLA and *dmdA* D/1 transcription) from phytoplankton activity (phytoplankton DLA). Overall, analyses suggest that elevated potential phytoplankton DMS production occurred under high UV-A conditions, while elevated bacterial DMSP demethylation occurred under low UV-A conditions, and elevated potential bacterial DMS production occurred under intermediate UV-A doses (Fig 7 & Table 1). These findings agree with previous suggestions that phytoplankton DMS production is enhanced by UV-A dose while bacterial DMSPd consumption is inhibited (Slezak et al., 2001; Sunda et al., 2002; Toole et al., 2006; Archer et al., 2010), and extend these hypotheses to suggest that bacterial DMSP cleavage may be UV-A tolerant.

It was hypothesized that bacterial DMSP demethylation would be the dominant pathway when DMSPd concentrations were low relative to bacterial carbon and sulfur demands (Kiene et al., 2000; Simó, 2001). However, no significant difference was found in DMSPd:bacterial carbon demand, TOC:bacterial carbon demand, or DMSPd:TOC in locations with elevated bacterial DMSP demethylation gene transcription relative to locations with elevated bacterial DMSP cleavage enzyme activity (student t-test, 95% confidence). Rather, the correlation analysis (Table 1) and MDS analysis (Fig. 7) suggest that both bacterial DMSP degradation pathways occur under elevated DMSPd and DMSPd:TOC concentrations. Findings further suggest that additional factors including light and temperature may play an important role in regulating the 'bacterial switch', based on observations that bacterial DMSP demethylation occurred under low UV-A dose whereas bacterial DMSP cleavage occurred under elevated temperatures and moderate UV-A dose. Previous studies have suggested that phytoplankton cleave DMSP to DMS as an anti-oxidant response to UV radiation (Sunda et al., 2002; Archer et al., 2010). The prevalence of the less energetically favorable bacterial DMSP cleavage pathway in moderate or high light environments may thus be related to reactive oxygen scavenging capabilities of DMS (Sunda et al., 2002), or possibly to the production of additional reactive oxygen species during demethylation pathway reactions (S. Gifford*, personal comm.*). Many cultured members of the *Roseobacter* clade have been shown to both demethylate and cleave DMSP (Gonzalez et al., 2000), making production of DMS by this group particularly sensitive to regulation by environmental conditions. Thus our data suggests a relationship between UV-A dose and bacterial DMSP degradation that warrants further investigation.

Both phytoplankton and bacterial DLA were significantly positively correlated with DMS concentration (Table 1), indicating that both may be relevant sources of DMS to the water

column, and yet showed distinctly different variability over the 10 month time-series. In the mixed layer, 61% of the variability in vertically averaged DMS concentrations ($p=0.04$) and 42% of the temporal and spatial variability of DMS ($p=0.03$) could be explained using a simple linear model combining potential DMS production (phytoplankton DLA and bacterial DLA*DMSPd) and DMS consumption (bacterial DMS consumption and UV-A dose, a proxy for photolysis) (Fig. 8). Only 26% of the variability in mixed layer DMS concentrations could be explained when potential bacterial DMS production was not included ($p=0.11$), and in the period from August through October, 85% of surface DMS variability (0-20m) could be explained by potential bacterial DMS production alone ($p<0.01$). This suggests bacteria are important contributors to DMS production at BATS, and were particularly so during the late summer and early fall of 2008. Below the mixed layer, DMS concentrations were low (average $1.0 \pm 1.4$ nM) and significantly correlated with bacterial DMS consumption ($r^2=0.70$, $p<0.01$). In addition, the DMS loss rate constant ($day^{-1}$) below the mixed layer was significantly higher than the rate constant in the mixed layer ($p<0.01$). This indicates a tight coupling between production and loss processes in deeper waters that makes it difficult to predict DMS standing stocks.

Drivers of marine biogeochemical cycling are extremely complex and act on numerous scales. We anticipated that an interdisciplinary dataset could assist in teasing apart the bacterial contribution to water column DMS(P) dynamics that begin as changes in gene transcription but are manifested as biogeochemical rates. We conclude that a diverse bacterial community is active in cycling organic sulfur in the Sargasso Sea; that in the late summer and fall, bacteria are important contributors to DMS production; that solar radiation, in particular UV-A dose, plays an important regulatory role in upper ocean sulfur cycling by both phytoplankton and bacteria; and that bacterial DMSP demethylation may be UV-A intolerant while bacterial DMS production

318 may be UV-A tolerant. Continued characterization of these factors through a combination of
319 physical, chemical, and molecular biological observations will improve our understanding of the
320 role of bacteria in DMS(P) cycling in the surface ocean and yield improved predictions of future
321 DMS emissions.
322

323 **EXPERIMENTAL PROCEDURES**

324 **Study site and sample collection**

325 The Bermuda Atlantic Time-series Study (BATS) site is located at 31°40'N 64°10'W.
326 Samples were collected on 10 monthly cruises to BATS between February and November 2008
327 (*Supplemental Material S3)*. Triplicate samples for functional gene analyses were collected at 0
328 m, 20 m, 40 m, and 60 m. Duplicate samples for DMS and DMSP (DMS(P)) concentrations,
329 DMS(P) turnover rates, and DMSP lyase potential enzyme activity (DLA) measurements were
330 collected at the above 4 depths plus 10 m and 100 m. All samples were collected before sunrise,
331 between 5 AM and 7 AM local time, to avoid the influence of diurnal variability (with the
332 exception of September where samples were collected at 3 AM) and processed immediately.
333 Functional gene and DLA samples were collected in 4 L acid-washed Nalgene® carboys.
334 Functional gene samples were filtered onto 47 mm diameter 0.2 μm pore-size polycarbonate
335 filters under low pressure (<0.02 Pa). The filters were changed every 30 minutes for DNA
336 samples and every 15 minutes for RNA samples to minimize sample degradation. On average,
337 3.6 L of seawater per DNA sample and 2.5 L of seawater per RNA sample were collected onto
338 four filters. After each collection, the RNA and DNA filters were immediately flash frozen in

339 liquid nitrogen. All functional gene samples were kept in liquid nitrogen or -80°C until they were
340 processed.

341 For the phytoplankton DLA assay, 500 ml of whole seawater was collected on autoclaved
342 25 mm diameter GF/C glass fiber filters (Whatman, pore-size ~1.2 μm) using gentle filtration
343 (<0.02 Pa). For the bacterial DLA assay, samples were gravity filtered through a 47 mm diameter
344 GF/C glass fiber filter (Whatman, pore-size ~1.2 μm) using a gentle flow to minimize
345 phytoplankton cells lysis during filtration. A total of 325 - 400 ml of GF/C pre-filtered water
346 (volumes were adjusted to maintain a filtration time of ~ 30 minutes) was then collected on
347 autoclaved 25 mm diameter 0.2 μm pore-size polycarbonate filters using gentle filtration (<0.02
348 Pa). As a result of extensive testing of the sampling protocol on the measured enzyme activity,
349 only changes in phytoplankton DLA greater than 0.20 nmol $L^{-1}$ $min^{-1}$ and bacterial DLA greater
350 than 0.16 nmol $L^{-1}$ $min^{-1}$ were considered robust (*Supplementary material S4*). This threshold is
351 significantly lower than the variability observed in both phytoplankton and bacterial DLA over
352 the 10 month time-series.
353

354 **Concentration and rate measurements**

355 DMS concentrations were determined using a purge and trap method modified from
356 Zemmelink *et al.* (2006). Briefly, sulfur gases were sparged from a 4 ml water sample with air or
357 nitrogen gas and trapped using a Carbopack-X trap in Sulfinert-treated 1/8" OD stainless steel
358 tubing. The trapped gases were analyzed on a gas chromatograph (GC) using an Alltech AT-
359 Sulfur capillary 0.32 mm ID column with an OI Corp. pulsed flame photometric detector
360 (PFPD). Total DMSP and DMSPd were quantified following the protocols described in Slezak *et*
361 *al*. (2007) and references therein. Particulate DMSP (DMSPp) was calculated as the difference

between total DMSP and DMSPd. Bacterial DMSPd and DMS consumption rates were determined using the $^{35}S$ tracer methods of Kiene and Linn (2000). These methods quantify the turnover rates of the DMSPd and DMS pools by measuring the loss of $^{35}S$-DMSPd and $^{35}S$-DMS from the dissolved and volatile pools, respectively. $^{35}S$-DMSPd and $^{35}S$-DMS were added at non-perturbing tracer levels of less than 0.05 nM. In addition, monthly depth profiles of bacterial carbon demand were determined using $^{3}H$-leucine incorporation following the protocol of Smith and Azam (1992). Leucine incorporation was converted to bacterial carbon demand using conversion factors from Carlson *et al*. (1996).

Ancillary measurements made by BATS scientists and utilized in this study include: temperature (°C), total organic carbon (TOC) (mol $kg^{-1}$), Turner Chlorophyll a (μg/kg), HPLC-determined pigments (ng $kg^{-1}$) and bacterial cell counts identified by 4',6-diamidino-2-phenylindole (DAPI) staining (cells $L^{-1}$) (http://bats.bios.edu download date 2011, Knap et al., 1997; Steinberg et al., 2001). Additional Chlorophyll a measurements were provided by the Bermuda Bio-Optics Project (N. McDonald *personal comm*., Siegel et al., 2001). The bioavailable fraction of TOC was assumed to equal semi-labile TOC, defined as total TOC minus the mean TOC concentration measured at depths greater than 3000 m (Carlson et al., 1994). Unless otherwise specified, we refer to the semi-labile TOC fraction simply as TOC.

Monthly vertical profiles of spectral downwelling irradiance for 10 wavelengths (324 nm – 665 nm) were taken using a Satlantic SeaWiFS profiling multi-channel radiometer (SPMR) coupled with a continuously sampling SeaWiFS multi-channel surface reference (SMSR). The data were collected and processed by the University of California, Santa Barbara (UCSB) Bermuda Bio-Optics Project (Siegel et al., 2001). Due to rapid convection in the mixed layer, the light dose experienced by organisms in this region was assumed to be uniform and was estimated

as the depth-weighted average of the observed light doses over the mixed layer (MLD), defined as the minimum depth where the potential density ($\sigma_\theta$) is greater than the potential density calculated using surface water salinity and surface temperature minus 0.2°C. In addition, we define moderate to high light environments as those with greater than 20% of the average summer surface incident UV-A (0.015 W $m^{-2}$).

**Gene abundance and transcription**

DNA samples were extracted using a phenol:chloroform extraction protocol (modified from Giovannoni et al., 1990; R. Parsons, BIOS, *personal comm*.) and described in detail in Levine (2010). DNA concentrations ranged from 0.1 μg per liter seawater filtered to 2.1 μg per liter seawater filtered with an average percent deviation between the biological triplicates of 21%.

RNA samples were extracted using the Qiagen® RNeasy Mini Kit™ adapted for environmental samples; a complete description is provided in Levine (2010). An initial on-column digestion using the Qiagen® RNase-free DNase Set™ and a second digestion using the Ambion® TURBO DNA-free™ kit were conducted to eliminate DNA contamination. RNA concentrations ranged from 10 ng per liter seawater filtered to 449 ng per liter seawater filtered with an average percent deviation between the biological triplicates of 26%.

Abundance and transcription of DMSP degradation genes were quantified using qPCR on a Bio-Rad iCycler iQ™. Five non-degenerate *dmdA* primer sets designed to target subclades A/1, A/2, C/2, D/1, and D/3 (Varaljay et al., 2010) and a degenerate *dddP* primer set targeting Group 1 (dddP_874F :5'- AAYGAAATWGTTGCCTTTGA -3 and dddP_971R: 5'-GCATDGCRTAAATCATATC-3`) designed by E. Howard (*personal comm.*) were used. *dmdA*

408 primer specificity was previously confirmed (Varaljay et al., 2010) and *dddP* specificity was
409 confirmed using Sanger sequencing on environmental samples from BATS DNA.

410 The qPCR cycle specifications and primer specific annealing temperatures are given in
411 s*upplementary material S5.* Gene abundance was quantified for all 5 *dmdA* subclades (A/1, A/2,
412 C/2, D/1, and D/3) and *dddP* using 12.5 μl Bio-Rad's iQ™ SYBR® Green 2X Supermix, 300
413 nM final primer concentrations, 2.5 μl Bovine Serum Albumin (BSA, final concentration 500 ng
414 $\mu l^{-1}$, New England Biolabs), and 3.0 μl of template in a 25.0 μl final reaction volume. Technical
415 duplicates (same sample) of biological triplicates (same time and depth but processed
416 independently) were analyzed, yielding 6 reactions per sample. Gene transcription was
417 quantified for *dddP* and *dmdA* subclades A/1, D/1, and D/3 with Bio-Rad's iScript One-Step RT-
418 PCR with SYBR® Green kit using the same concentrations as above except 5.0 μl of template
419 was used and 2.5 μl T4gp32 (final concentration 10 ng $\mu l^{-1}$, Roche Diagnostics GmbH) was used
420 in place of BSA. Technical duplicates of biological duplicates (N=4) and a reverse-transcriptase
421 enzyme control (-RT) were run for each sample with each primer set to confirm the absence of
422 contaminating DNA. The addition of BSA or T4gp32 eliminated PCR inhibition (*Supplementary*
423 *material S6*).

424 Ten-fold serially diluted standard curves covering the sample range were run in duplicate
425 on each plate. Standards were made from PCR products from environmental DNA cloned into
426 the PCR 2.1 or PCR 4.0 vector using the TOPO TA Cloning® kit (Invitrogen) and were
427 quantified based on the length of the amplicon insert and the concentration. Triplicate no-
428 template controls were run on every plate.

429 A single peak was confirmed from melt curve analysis for all primers, and qPCR
430 products were verified by agarose gel. Samples with transcript numbers greater than one standard

deviation above the mean were marked as "elevated transcription". Some samples analyzed for the transcription of subclade *dmdA* A/1 and *dddP* showed non-specific amplification by melt curve analysis, most likely due to low initial gene copy number. Samples with multiple melting curve peaks but with at least one peak at the correct melting temperature (compared to the standard clone melt curve) were marked as non-quantifiable "transcription present". Of the 40 samples analyzed for subclade A/1 transcription, 11 samples showed specific amplification, and 21 were marked as "transcription present". *dddP* transcript numbers were too low in all 40 samples for a quantitative analysis of copy number; however, 8 samples were marked as "transcription present".

The PCR efficiency of the environmental samples was shown to be within error of the efficiency of the standards using the LinRegPCR program (Ramakers et al., 2003; Ruijter et al., 2009). Gene abundance and transcription data are presented as copies $L^{-1}$ of seawater filtered. RNA samples with DNA contamination greater than 3% of the RNA signal were discarded. Of RNA samples with quantifiable or qualitative transcription, only one sample analyzed (for subclade D/1 transcription) was discarded due to DNA contamination.

**DMSP lyase activity**

The methods of Harada *et al.* (2004) and Steinke *et al.* (2000), developed to measure the activity of the phytoplankton DMSP lyase pathway, were applied to two operationally defined fractions: phytoplankton (>1.2 μm) and bacterial (0.2 μm - 1.2 μm). The protocol following filtration (*see above*) was identical for both size fractions and is described in detail in Levine (2010). Briefly, the filter was placed in a 14 ml amber glass serum vial containing 1 ml of 200 mM Tris buffer (pH 8) with 500 mM NaCl. The vial was vortexed and incubated for 20 minutes.

This effectively lyses phytoplankton cells (Steinke et al., 2000) but is not stringent enough to lyse bacterial cells (*Supplementary material S7)*. Following the incubation, a saturating concentration of DMSP was added (final concentration 5 mM) and the vial was immediately crimped. The evolution of DMS in each vial was analyzed using focused headspace samples on the GC system described above. Five time-points were measured per sample over an 18 minute interval. A short measurement period was chosen to negate the possibility of enzyme induction. This was confirmed by laboratory and field tests that showed a linear increase in DMS concentrations over the first 30 minutes of the DLA assay.

Enzyme activity is temperature dependent; therefore, all DLA measurements were made at the MLD temperature using an under-way seawater bath to best approximate in situ conditions. Assay temperatures ranged from 21° - 26.5°C over the 10 month time-series. The difference between the DLA assay temperature and the 100 m water temperature ranged from < 1°C in February to 6.5°C in August and September. The DLA assay most likely overestimates enzyme activity at depth in the summer due to this temperature difference; however, this overestimation is only on the order of 20% (*Supplementary material S4*).

DMS concentrations were quantified using a standard curve defined by diluting pure DMS in aqueous solutions (0.5- 10 μM). The DLA rate was calculated as:

$$DLA_{PotentialActivity} = \left[\left(\frac{dDMS}{dt}\right) - \left(\frac{dDMSP_{abiotic}}{dt}\right)\right] \Big/ Vol \qquad (1)$$

where $\frac{dDMS}{dt}$ is the slope of the best-fit trend line to the observed change in DMS with time, $\frac{dDMSP_{abiotic}}{dt}$ is the correction for the abiotic degradation of DMSP in the assay (*Supplementary material S8*), and *Vol* is the volume of seawater filtered. The $r^2$ of the $\frac{dDMS}{dt}$ trend line was typically 0.99 or better. The potential DLA for each depth was calculated as the average of the duplicate samples. An additional correction was applied to bacterial DLA samples to account for the effect of the polycarbonate filter on the observed DMS concentrations (*Supplementary material S8*).

Potential enzyme assays measure the non-substrate limited activity of the enzymes that is assumed to be proportional to the enzyme concentration in solution. In order to better estimate rates of bacterial DMS production, the observed bacterial DLA was multiplied by the in situ DMSPd concentration as bacteria are dependent on external sources of DMSP. However, the conclusions of this study remain unchanged if the analyses are conducted using bacterial DLA alone. A similar correction for the phytoplankton DLA activity was not made as the intracellular concentration of DMSPp in DMS-producing cells may not be linearly related to total water column DMSPp concentration due to significant, species-specific, variability in DMSP production and DMSP lyase enzyme concentration (e.g. Keller et al., 1989; Matrai and Keller, 1994).

**Statistical analysis**

To investigate potential environmental drivers of DMSP degradation and DMS production, linear relationships between a suite of physical, chemical and biological factors and

gene abundance, expression, and DLA were investigated. Specifically, DMS, DMSPp, DMSPd, and TOC concentrations, DMSP:TOC, DMSP consumption, Chlorophyll a, bacterial carbon demand, bacterial abundance, temperature, depth, 340 nm light dose (UV-A), 490 nm light dose, and 684 nm light dose were used. The Results and Discussion sections focus on the environmental variables most significantly correlated with changes in sulfur cycling.

A non-metric multidimensional scaling (MDS) analysis was conducted using R's Vegan package (Oksanen et al., 2010) to further investigate potential drivers of DMSP degradation gene abundance. Gene abundance data were log-transformed and normalized as a fraction of the highest value. The Bray-Curtis method was used to calculate dissimilarity indices and 4 dimensions were chosen as additional dimensions resulted in minimal increases in the goodness of fit, calculated as Kruskal's Stress (formula I). For each axis of variability, the MDS analysis yielded sample scores for each sample and the projection or weighting of each gene data set on that axis (variable score). The axis sample scores were then linearly regressed against a suite of physical and chemical observations (*see above*) to investigate potential sources of variation. In addition, the day of the year was used to determine the impact of season on the distribution of bacterial DMSP genes.

A second MDS analysis was performed as described above to further investigate potential the mechanisms driving variability in DMSP degradation and DMS production. Here *dmdA* D/1 gene transcription, potential bacterial DMS production (DLA*DMSPd), and potential phytoplankton DMS production (DLA) were used. Each data set was normalized to range from zero to one before the analysis was performed.

**ACKNOWLEDGEMENTS:**

We would like to acknowledge Aimee Neeley and Erinn Howard for significant contributions to this work, D. Siegel and D. Court for assistance with the solar radiation data, the staff at the Bermuda Institute of Ocean Sciences, and the captain and crew of the *R/V Atlantic Explorer*. This research was funded by National Science Foundation (NSF) grants OCE-0525928, OCE-072417, and OCE-042516. Additional funding was provided by the NSF Center for Microbial Oceanography Research and Education (CMORE), the Gordon and Betty Moore Foundation, the Scurlock Fund, the Ocean Ventures Fund, a National Defense Science and Engineering Graduate Fellowship, and an Environmental Protection Agency STAR Graduate Fellowship.

527

528 **REFERENCES**


529 Archer, S.D., Ragni, M., Webster, R., Airs, R.L., and Geider, R.J. (2010) Dimethyl
530 sulfoniopropionate and dimethyl sulfide production in response to photoinhibition in Emiliania
531 huxleyi. *Limnology and Oceanography* **55**: 1579-1589.

532 Bates, T.S., Kiene, R.P., Wolfe, G.V., Matrai, P.A., Chavez, F.P., Buck, K.R. et al. (1994) The
533 cycling of sulfur in surface seawater of the Northeast Pacific. *Journal of Geophysical Research-*
534 *Oceans* **99**: 7835-7843.

535 Bell, T.G., Malin, G., Kim, Y.N., and Steinke, M. (2007) Spatial variability in DMSP-lyase
536 activity along an Atlantic meridional transect. *Aquatic Sciences* **69**: 320-329.

537 Cantoni, G.L., and Anderson, D.G. (1956) Enzymatic cleavage of dimethylpropiothetin by
538 polysiphonia lansoa. *Journal of Biological Chemistry* **222**: 171-177.

539 Carlson, C.A., Ducklow, H.W., and Michaels, A.F. (1994) Annual flux of dissolved organic-
540 carbon from the euphotic zone in the northwestern Sargasso Sea. *Nature* **371**: 405-408.

541 Carlson, C.A., Ducklow, H.W., and Sleeter, T.D. (1996) Stocks and dynamics of
542 bacterioplankton in the northwestern Sargasso Sea. *Deep-Sea Research Part II-Topical Studies*
543 *in Oceanography* **43**: 491-515.

544 Carlson, C.A., Morris, R., Parsons, R., Treusch, A.H., Giovannoni, S.J., and Vergin, K. (2009)
545 Seasonal dynamics of SAR11 populations in the euphotic and mesopelagic zones of the
546 northwestern Sargasso Sea. *ISME Journal* **3**: 283-295.

547 Charlson, R.J., Lovelock, J.E., Andreae, M.O., and Warren, S.G. (1987) Oceanic phytoplankton,
548 atmospheric sulfur, cloud albedo and climate. *Nature* **326**: 655-661.

549 Curson, A.R.J., Sullivan, M.J., Todd, J.D., and Johnston, A.W.B. (2011) DddY, a periplasmic
550 dimethylsulfoniopropionate lyase found in taxonomically diverse species of Proteobacteria.
551 *ISME Journal* **5**: 1191-1200.

552 Curson, A.R.J., Rogers, R., Todd, J.D., Brearley, C.A., and Johnston, A.W.B. (2008) Molecular
553 genetic analysis of a dimethylsulfoniopropionate lyase that liberates the climate-changing gas
554 dimethylsulfide in several marine alpha-proteobacteria and Rhodobacter sphaeroides.
555 *Environmental Microbiology* **10**: 757-767.

556 Dacey, J.W.H., Howse, F.A., Michaels, A.F., and Wakeham, S.G. (1998) Temporal variability of
557 dimethylsulfide and dimethylsulfoniopropionate in the Sargasso Sea. *Deep-Sea Research Part I-*
558 *Oceanographic Research Papers* **45**: 2085-2104.

559 Gifford, S.M., Sharma, S., Rinta-Kanto, J.M., and Moran, M.A. (2011) Quantitative analysis of a
560 deeply sequenced marine microbial metatranscriptome. *ISME Journal* **5**: 461-472.

561 Giovannoni, S.J., Delong, E.F., Schmidt, T.M., and Pace, N.R. (1990) Tangential Flow Filtration
562 and Preliminary Phylogenetic Analysis of Marine Picoplankton. *Applied and Environmental*
563 *Microbiology* **56**: 2572-2575.

564 Gonzalez, J.M., Simó, R., Massana, R., Covert, J.S., Casamayor, E.O., Pedrós-Alió, C., and
565 Moran, M.A. (2000) Bacterial community structure associated with a
566 dimethylsulfoniopropionate-producing North Atlantic algal bloom. *Applied and Environmental*
567 *Microbiology* **66**: 4237-4246.

568 Harada, H., Rouse, M.A., Sunda, W., and Kiene, R.P. (2004) Latitudinal and vertical
569 distributions of particle-associated dimethylsulfoniopropionate (DMSP) lyase activity in the
570 western North Atlantic Ocean. *Canadian Journal of Fisheries and Aquatic Sciences* **61**: 700-711.

571 Howard, E.C., Sun, S.L., Biers, E.J., and Moran, M.A. (2008) Abundant and diverse bacteria
572 involved in DMSP degradation in marine surface waters. *Environmental Microbiology* **10**: 2397-
573 2410.

574 Howard, E.C., Henriksen, J.R., Buchan, A., Reisch, C.R., Buergmann, H., Welsh, R. et al. (2006)
575 Bacterial taxa that limit sulfur flux from the ocean. *Science* **314**: 649-652.

576 Keller, M.D., Bellows, W.K., and Guillard, R.R.L. (1989) Dimethylsulfide production in marine
577 phytoplankton. In *Biogenic sulfur in the environment*. Saltzman, E.S., and Cooper William, W.J.
578 (eds). Washington, D.C.: ACS Symposium Series, American Chemical Society, pp. 167-182.

579 Kiene, R.P. (1996) Production of methanethiol from dimethylsulfoniopropionate in marine
580 surface waters. *Marine Chemistry* **54**: 69-83.

581 Kiene, R.P., and Linn, L.J. (2000) The fate of dissolved dimethylsulfoniopropionate (DMSP) in
582 seawater: Tracer studies using S-35-DMSP. *Geochimica et Cosmochimica Acta* **64**: 2797-2810.

583 Kiene, R.P., Linn, L.J., and Bruton, J.A. (2000) New and important roles for DMSP in marine
584 microbial communities. *Journal of Sea Research* **43**: 209-224.

585 Knap, A.H., Michaels, A.F., Steinberg, D.K., Bahr, F., Bates, N.R., Bell, S. et al. (1997)
586 Bermuda Atlantic Time-series Study Methods Manual Version 4.

587 Kwint, R.L.J., and Kramer, K.J.M. (1996) Annual cycle of the production and fate of DMS and
588 DMSP in a marine coastal system. *Marine Ecology-Progress Series* **134**: 217-224.

589 Ledyard, K.M., Delong, E.F., and Dacey, J.W.H. (1993) Characterization of a DMSP-degrading
590 bacterial isolate from the Sargasso Sea. *Archives of Microbiology* **160**: 312-318.

591 Levine, N.M. (2010) Understanding the ocean carbon and sulfur cycles in the context of a
592 variable ocean : a study of anthropogenic carbon storage and dimethylsulfide production in the
593 Atlantic Ocean. In *Chemical Oceanography*. Woods Hole: MIT-WHOI Joint Program, p. 298.

594 Malmstrom, R.R., Kiene, R.P., and Kirchman, D.L. (2004a) Identification and enumeration of
595 bacteria assimilating dimethylsulfoniopropionate (DMSP) in the North Atlantic and Gulf of
596 Mexico. *Limnology and Oceanography* **49**: 597-606.

597 Malmstrom, R.R., Kiene, R.P., Cottrell, M.T., and Kirchman, D.L. (2004b) Contribution of
598 SAR11 bacteria to dissolved dimethylsulfoniopropionate and amino acid uptake in the North
599 Atlantic ocean. *Applied and Environmental Microbiology* **70**: 4129-4135.

600 Matrai, P.A., and Keller, M.D. (1994) Total organic sulfur and dimethylsulfoniopropionate in
601 marine-phytoplankton - intracellular variations. *Marine Biology* **119**: 61-68.

602 Oksanen, J., Blanchet, F.G., Kindt, R., Legendre, P., O'Hara, R.B., Simpson, G.L. et al. (2010)
603 In: vegan: Community Ecology Package. R package version 1.17-3. http://CRAN.R-
604 project.org/package-vegan.

605 Ramakers, C., Ruijter, J.M., Deprez, R.H.L., and Moorman, A.F.M. (2003) Assumption-free
606 analysis of quantitative real-time polymerase chain reaction (PCR) data. *Neuroscience Letters*
607 **339**: 62-66.

608 Ruijter, J.M., Ramakers, C., Hoogaars, W.M.H., Karlen, Y., Bakker, O., van den Hoff, M.J.B.,
609 and Moorman, A.F.M. (2009) Amplification efficiency: linking baseline and bias in the analysis
610 of quantitative PCR data. *Nucleic Acids Research* **37**: e45.

611 Shaw, G.E. (1983) Bio-controlled thermostasis involving the sulfur cycle. *Climatic Change* **5**:
612 297-303.

613 Siegel, D.A., Westberry, T.K., O'Brien, M.C., Nelson, N.B., Michaels, A.F., Morrison, J.R. et al.
614 (2001) Bio-optical modeling of primary production on regional scales: the Bermuda BioOptics
615 project. *Deep-Sea Research Part II-Topical Studies in Oceanography* **48**: 1865-1896.

616 Simó, R. (2001) Production of atmospheric sulfur by oceanic plankton: biogeochemical,
617 ecological and evolutionary links. *Trends in Ecology & Evolution* **16**: 287-294.

618 Simó, R., Archer, S.D., Pedrós-Alió, C., Gilpin, L., and Stelfox-Widdicombe, C.E. (2002)
619 Coupled dynamics of dimethylsulfoniopropionate and dimethylsulfide cycling and the microbial
620 food web in surface waters of the North Atlantic. *Limnology and Oceanography* **47**: 53-61.

621 Slezak, D., Brugger, A., and Herndl, G.J. (2001) Impact of solar radiation on the biological
622 removal of dimethylsulfoniopropionate and dimethylsulfide in marine surface waters. *Aquatic*
623 *Microbial Ecology* **25**: 87-97.

624 Slezak, D., Kiene, R.P., Toole, D.A., Simó, R., and Kieber, D.J. (2007) Effects of solar radiation
625 on the fate of dissolved DMSP and conversion to DMS in seawater. *Aquatic Sciences* **69**: 377-
626 393.

627 Smith, D.C., and Azam, F. (1992) A simple, economical method for measuring bacterial protein
628 synthesis rates in seawater using 3H-leucine. *Mar Microb Food Webs* **6**: 107-114.

629 Steinberg, D.K., Carlson, C.A., Bates, N.R., Johnson, R.J., Michaels, A.F., and Knap, A.H.
630 (2001) Overview of the US JGOFS Bermuda Atlantic Time-series Study (BATS): a decade-scale
631 look at ocean biology and biogeochemistry. *Deep-Sea Research Part II-Topical Studies in*
632 *Oceanography* **48**: 1405-1447.

633 Steinke, M., Malin, G., Turner, S.M., and Liss, P.S. (2000) Determinations of
634 dimethylsulphoniopropionate (DMSP) lyase activity using headspace analysis of
635 dimethylsulphide (DMS). *Journal of Sea Research* **43**: 233-244.

636 Steinke, M., Malin, G., Gibb, S.W., and Burkill, P.H. (2002) Vertical and temporal variability of
637 DMSP lyase activity in a coccolithophorid bloom in the northern North Sea. *Deep-Sea Research*
638 *Part II-Topical Studies in Oceanography* **49**: 3001-3016.

639 Sunda, W., Kieber, D.J., Kiene, R.P., and Huntsman, S. (2002) An antioxidant function for
640 DMSP and DMS in marine algae. *Nature* **418**: 317-320.

641 Taylor, B.F., and Gilchrist, D.C. (1991) New routes for aerobic biodegradation of
642 dimethylsulfoniopropionate. *Applied and Environmental Microbiology* **57**: 3581-3584.

643 Todd, J.D., Kirkwood, M., Newton-Payne, S., and Johnston, A.W.B. (2012) DddW, a third
644 DMSP lyase in a model Roseobacter marine bacterium, Ruegeria pomeroyi DSS-3. *ISME*
645 *Journal* **6**: 223-226.

646 Todd, J.D., Curson, A.R.J., Dupont, C.L., Nicholson, P., and Johnston, A.W.B. (2009) The dddP
647 gene, encoding a novel enzyme that converts dimethylsulfoniopropionate into dimethyl sulfide,
648 is widespread in ocean metagenomes and marine bacteria and also occurs in some Ascomycete
649 fungi. *Environmental Microbiology* **11**: 1376-1385.

650 Todd, J.D., Curson, A.R.J., Kirkwood, M., Sullivan, M.J., Green, R.T., and Johnston, A.W.B.
651 (2011) DddQ, a novel, cupin-containing, dimethylsulfoniopropionate lyase in marine
652 roseobacters and in uncultured marine bacteria. *Environmental Microbiology* **13**: 427-438.

653 Todd, J.D., Rogers, R., Li, Y.G., Wexler, M., Bond, P.L., Sun, L. et al. (2007) Structural and
654 regulatory genes required to make the gas dimethyl sulfide in bacteria. *Science* **315**: 666-669.

655 Toole, D.A., and Siegel, D.A. (2004) Light-driven cycling of dimethylsulfide (DMS) in the
656 Sargasso Sea: Closing the loop. *Geophysical Research Letters* **31**.

657 Toole, D.A., Kieber, D.J., Kiene, R.P., Siegel, D.A., and Nelson, N.B. (2003) Photolysis and the
658 dimethylsulfide (DMS) summer paradox in the Sargasso Sea. *Limnology and Oceanography* **48**:
659 1088-1100.

660 Toole, D.A., Slezak, D., Kiene, R.P., Kieber, D.J., and Siegel, D.A. (2006) Effects of solar
661 radiation on dimethylsulfide cycling in the western Atlantic Ocean. *Deep-Sea Research Part I-*
662 *Oceanographic Research Papers* **53**: 136-153.

663 Vallina, S.M., and Simó, R. (2007) Strong relationship between DMS and the solar radiation
664 dose over the global surface ocean. *Science* **315**: 506-508.

665 Varaljay, V., Giffford, S.M., Wilson, S.T., Sharma, S., Karl, D.M., and Moran, M.A. (submitted)
666 The Abundance and Diversity of Bacterial
667 Dimethylsulfoniopropionate-degrading Genes dmdA and dddP in the
668 Oligotropic North Pacific Subtropical Gyre.

669 Varaljay, V.A., Howard, E.C., Sun, S.L., and Moran, M.A. (2010) Deep sequencing of a
670 dimethylsulfoniopropionate-degrading gene (dmdA) by using PCR primer pairs designed on the
671 basis of marine metagenomic data. *Applied and Environmental Microbiology* **76**: 609-617.

672 Vila-Costa, M., Rinta-Kanto, J.M., Sun, S.L., Sharma, S., Poretsky, R., and Moran, M.A. (2010)
673 Transcriptomic analysis of a marine bacterial community enriched with
674 dimethylsulfoniopropionate. *ISME Journal* **4**: 1410-1420.

675 Yoch, D.C., Ansede, J.H., and Rabinowitz, K.S. (1997) Evidence for intracellular and
676 extracellular dimethylsulfoniopropionate (DMSP) lyases and DMSP uptake sites in two species
677 of marine bacteria. *Applied and Environmental Microbiology* **63**: 3182-3188.

678 Zemmelink, H.J., Houghton, L., Frew, N.M., and Dacey, J.W.H. (2006) Dimethylsulfide and
679 major sulfur compounds in a stratified coastal salt pond. *Limnology and Oceanography* **51**: 271-
680 279.
681
682
683

683 **Figure Captions:**

684 **Figure 1**: Seasonal cycle of vertically averaged mixed layer DMS concentration at BATS. The
685 mean seasonal cycle of mixed layer DMS concentrations averaged over 1992-1994 (Dacey et al.,
686 1998) is shown in the solid black line with the 1σ variation shown with gray shading. The
687 average mixed layer DMS concentrations for 2008 (*this study*) is shown as a black dashed line.
688 Note the influence of Hurricane Bertha during July 2008 resulting in atypically low mixed layer
689 DMS concentrations.

690

691 **Figure 2:** Variability in the upper ocean sulfur cycle at BATS in 2008. The concentrations of
692 DMS, DMSPp and DMSPd in nM are given in panels a, b and c, respectively. The UV-A light
693 dose (340 nm) is given in panel d. The rates of DMSPd and DMS consumption in nM $d^{-1}$ are
694 plotted in panels e and f, respectively. The thick solid gray lines indicate the mixed layer depth,
695 defined as the minimum depth where the potential density ($\sigma_\theta$) is greater than the potential
696 density calculated using surface water salinity and surface temperature minus 0.2°C. The thin
697 solid gray lines represent the 1σ variation of the mixed layer depth during the monthly cruise and
698 the dashed gray lines show the deepening of the mixed layer due to Hurricane Bertha.

699

700 **Figure 3:** The abundance of DMSP degradation genes at BATS. Panels a-e show the abundance
701 of *dmdA* subclades D/1, A/2, C/2, D/3, and A/1 in copies $L^{-1}$ of seawater, respectively. Panel f
702 plots the abundance of *dddP* in copies $L^{-1}$. The symbol color corresponds to the number of gene
703 copies $L^{-1}$. The average measurement error is 23%, with a range of 5% - 70%. Measurements
704 with an error greater than 25% are indicated with hash marks (e.g. D/1 March 60 m). Note the
705 more than two orders of magnitude variation in color bar scales. The solid gray lines indicate the

706 mixed layer depth and the dashed gray lines show the deepening of the mixed layer due to
707 Hurricane Bertha.
708
709 **Figure 4:** Transcription of DMSP degradation genes at BATS. Transcript number for *dmdA*
710 subclades D/1, D/3, and A/1 and *dddP* in copies $L^{-1}$ are plotted in panels a-d, respectively. The
711 symbol color corresponds to the number of transcript copies $L^{-1}$. The average measurement error
712 is 37%, with a range of 0.5% - 140%. Measurements with an error greater than 55% are
713 indicated with hashed marks (e.g. D/1 March 0 m). Samples marked as "transcription present"
714 are denoted by + symbols. Black open circles denote samples with no detectable transcription.
715 The solid gray lines indicate the mixed layer depth and the dashed gray lines show the deepening
716 of the mixed layer due to Hurricane Bertha.
717
718 **Figure 5:** Phytoplankton and bacterial DMSP lyase potential enzyme activity. Panel a shows the
719 potential phytoplankton DMS production as determined by the phytoplankton DMSP lyase
720 potential enzyme activity. Panel b shows potential bacterial DMS production estimated from
721 bacterial DMSP lyase activity and dissolved DMSPd concentrations. Sample locations for
722 transcription analysis are shown as white dots and the locations with *dddP* transcripts present are
723 denoted with black squares. The solid gray lines indicate the mixed layer depth and the dashed
724 gray lines show the deepening of the mixed layer due to Hurricane Bertha.
725
726 **Figure 6**: Multi-dimensional scaling plot of Group I and Group II gene abundance. The first and
727 second axis scores for all samples (N=40) and the variable scores for *dmdA* A/1, A/2, D/1, and
728 D/3 and *dddP* are displayed. Samples are shaded according to season: winter (Feb – Mar), spring

729 (Apr – May), summer (June – Sept), and fall (Oct – Nov). July samples are plotted as open black
730 circles and May samples from 40 m and 60 m are plotted as open gray triangles. The samples
731 cluster into two groups, Group I with high A/1, D/3, and *dddP* copy numbers and Group II with
732 high A/2 and D/1 copy numbers.
733
734 **Figure 7:** Multi-dimensional scaling plot showing the relationship between DMSP degradation
735 and UV-A light dose. The variable scores for *dmdA* D/1 transcription, phytoplankton enzyme
736 activity, and bacterial enzyme activity are also shown. Each symbol is shaded according to the
737 light UV-A dose experienced by that sample, with moderate to high light defined as a light dose
738 above 20% of the average summer surface incident UV-A (0.015 W $m^{-2}$) and low light defined
739 as a light dose below this value.
740
741 **Figure 8**: Observed versus predicted DMS concentrations. Panel a shows observed mixed layer
742 DMS concentrations. Panel b shows predicted mixed layer DMS concentrations based on a
743 linear regression against potential phytoplankton DMS production, potential bacterial DMS
744 production (DLA*DMSPd), bacterial DMS consumption, and UV-A dose (which we use here as
745 a proxy for photolysis). The solid gray lines indicate the mixed layer depth and the gray circles
746 indicate sample locations. The prediction explains 42% of the observed temporal and spatial
747 variability in mixed layer DMS concentrations. February, April and November DMS values
748 could not be estimated due to missing light or rate data.

**Table 1:** Correlation between DMSP degradation (*dmdA* transcription and enzyme activity) and observed chemical, physical, and biological parameters. For each relationship, the number of data points (n), the linear correlation coefficient (r) and p value are given. Correlation coefficients with p values greater than 0.05 are designated non-significant (*ns*). The percentage of elevated transcription or activity occurring under moderate to high UV-A dose is also given, where elevated transcription or enzyme activity is defined as greater than 1σ above the mean and moderate to high UV-A dose is defined as greater than 20% of summer surface incident UV-A.

| | n[a] | *dmdA* D/1 transcription | Bacterial DLA | Bacterial DLA x DMSPd | Phytoplankton DLA |
|---|---|---|---|---|---|
| **Temperature** | 60 (26) | *ns* | 0.54 (<0.01) | 0.44 (<0.01) | 0.39 (<0.01) |
| **Month** | 60 (26) | *ns* | 0.48 (<0.01) | 0.48 (<0.01) | *ns* |
| **UV-A dose** | 48 (22) | -0.55 (<0.01)[b] | *ns* | *ns* | 0.55 (<0.01)[c] |
| **DMS** | 60 (26) | -0.56 (<0.01) | 0.41 (<0.01) | 0.27 (0.04) | 0.53 (<0.01) |
| **DMSPd** | 60 (26) | 0.43 (0.03) | 0.25 (0.05) | 0.51 (<0.01) | 0.35 (<0.01) |
| **DMSPp** | 60 (26) | *ns* | *ns* | 0.35 (<0.01) | 0.33 (<0.01) |
| **TOC** | 59 (25) | -0.43 (0.03) | 0.33 (0.01) | 0.29 (0.03) | 0.57 (<0.01) |
| **DMSPd/TOC** | 59 (25) | 0.46 (0.02) | *ns* | 0.47 (<0.01) | 0.29 (0.03) |
| **DMS consumption** | 54 (22) | -0.44 (0.04) | *ns* | *ns* | 0.40 (<0.01) |
| **Bacterial Carbon Demand** | 60 (26) | *ns* | -0.36 (<0.01) | -0.30 (0.02) | *ns* |
| **Amount of Elevated Expression Occurring Under Moderate to High UV-A** | | 14% (1 of 7) | 67% (4 of 6) | 33% (2 of 6) | 88% (7 of 8) |

[a] Number of samples used in the correlation. The number in parenthesis is the number used for the *dmdA* D/1 transcription correlation (column 3).

[b] The correlation with ln(UV-A) is r=-0.67, p<0.01

[c] The correlation with ln(UV-A) is r=0.40, p<0.01

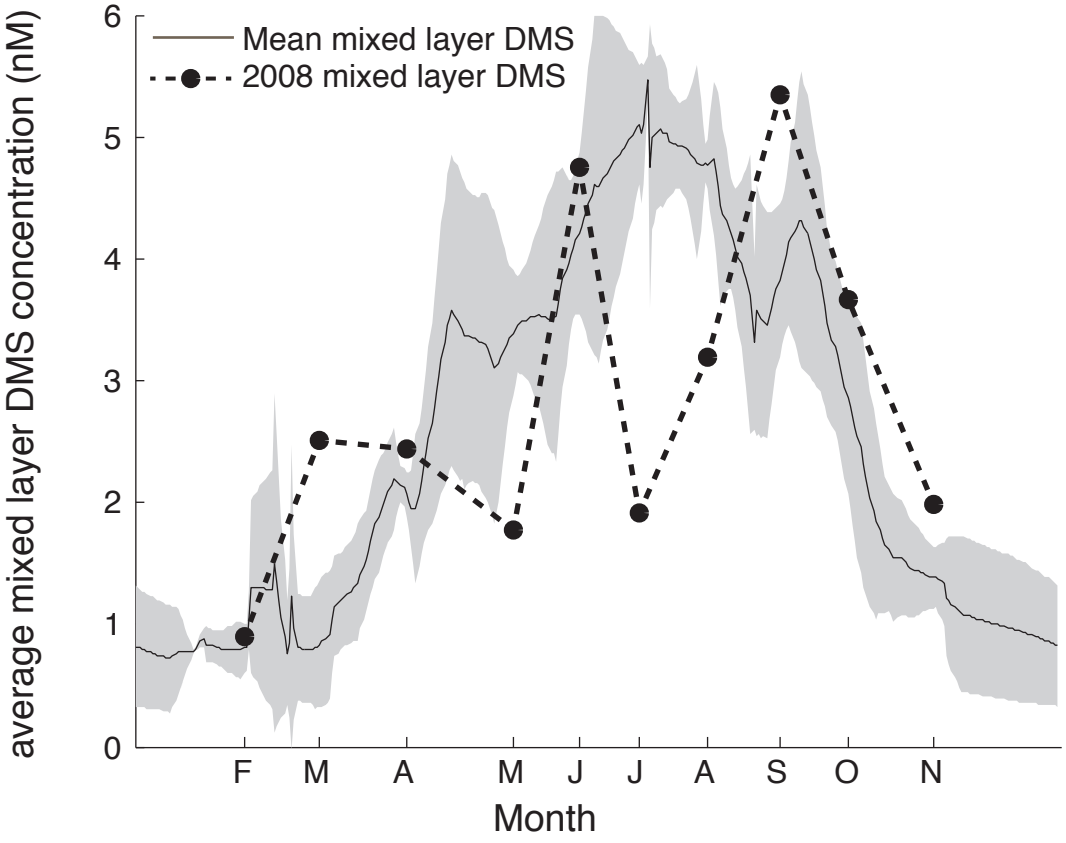
Mean mixed layer DMS
2008 mixed layer DMS
average mixed layer DMS concentration (nM)
0
1
2
3
4
5
6
F
M
A
M
J
J
A
S
O
N
Month

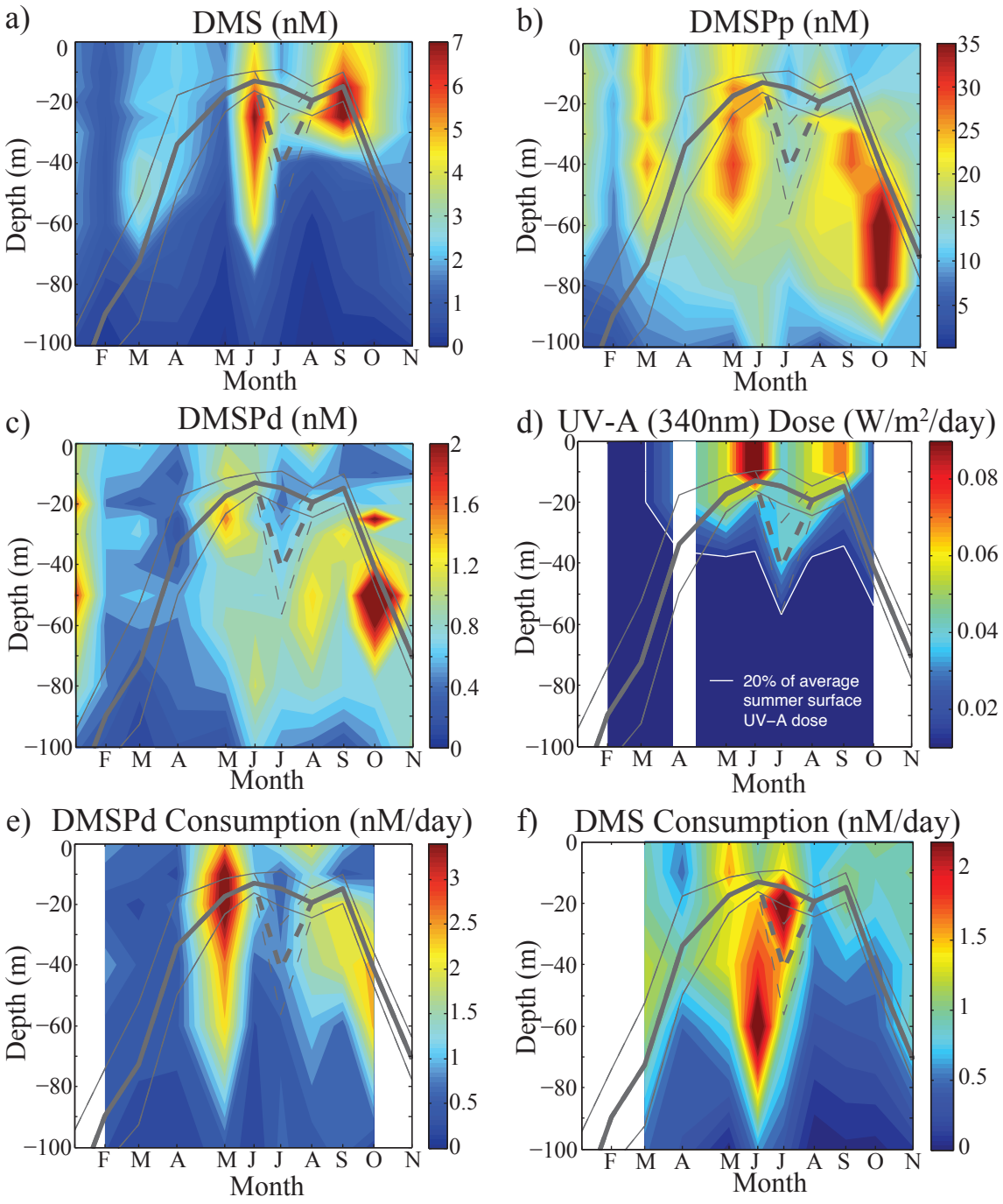
a)
DMS (nM)
b)
DMSPp (nM)
c)
DMSPd (nM)
d) UV-A (340nm) Dose (W/m²/day)
20% of average summer surface UV–A dose
e) DMSPd Consumption (nM/day)
f) DMS Consumption (nM/day)
Depth (m)
Month
F M A M J J A S O N

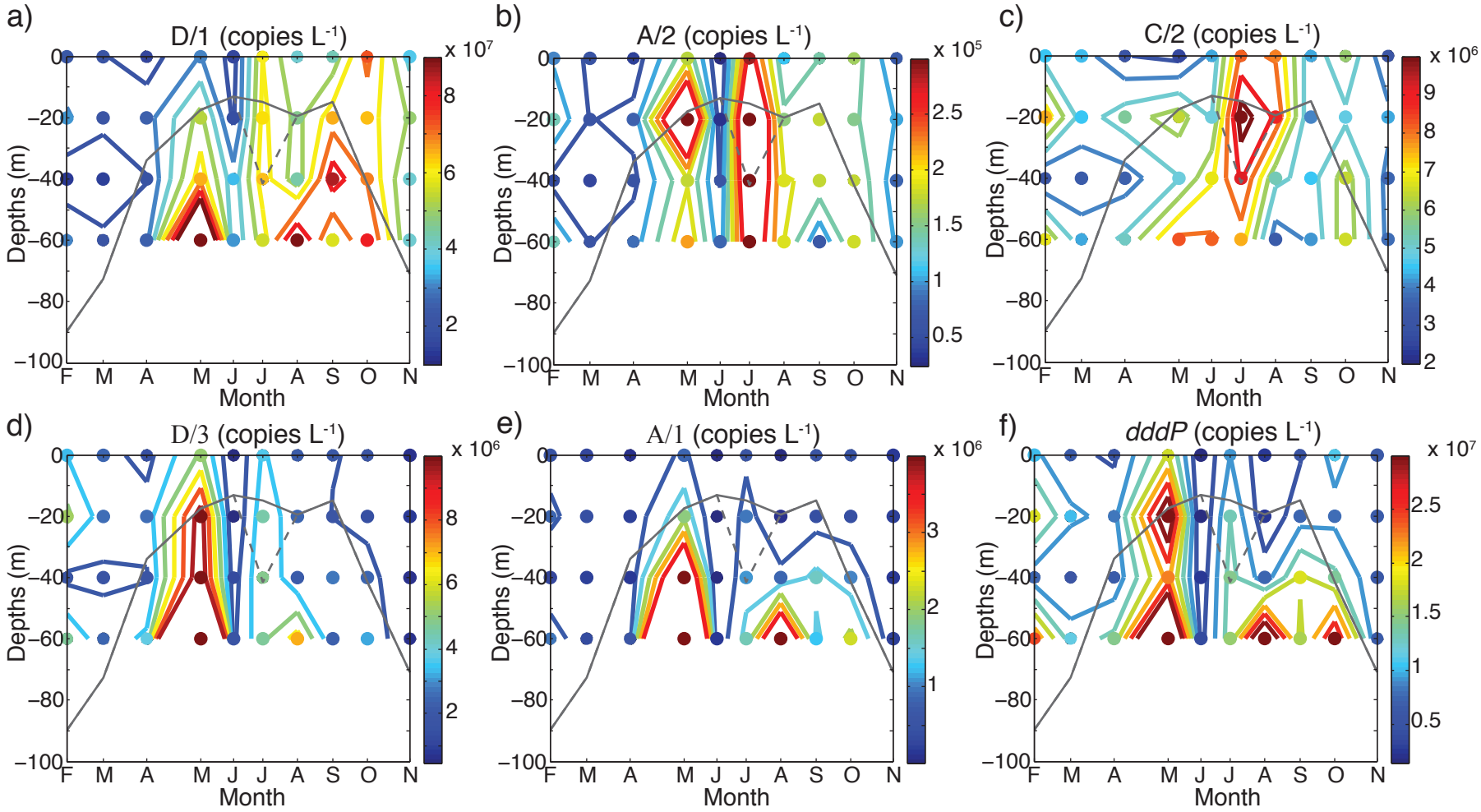
a)
D/1 (copies L-1)
x 10^7
b)
A/2 (copies L-1)
x 10^5
c)
C/2 (copies L-1)
x 10^6
d)
D/3 (copies L-1)
x 10^6
e)
A/1 (copies L-1)
x 10^6
f)
dddP (copies L-1)
x 10^7
Depths (m)
Month
F M A M J J A S O N

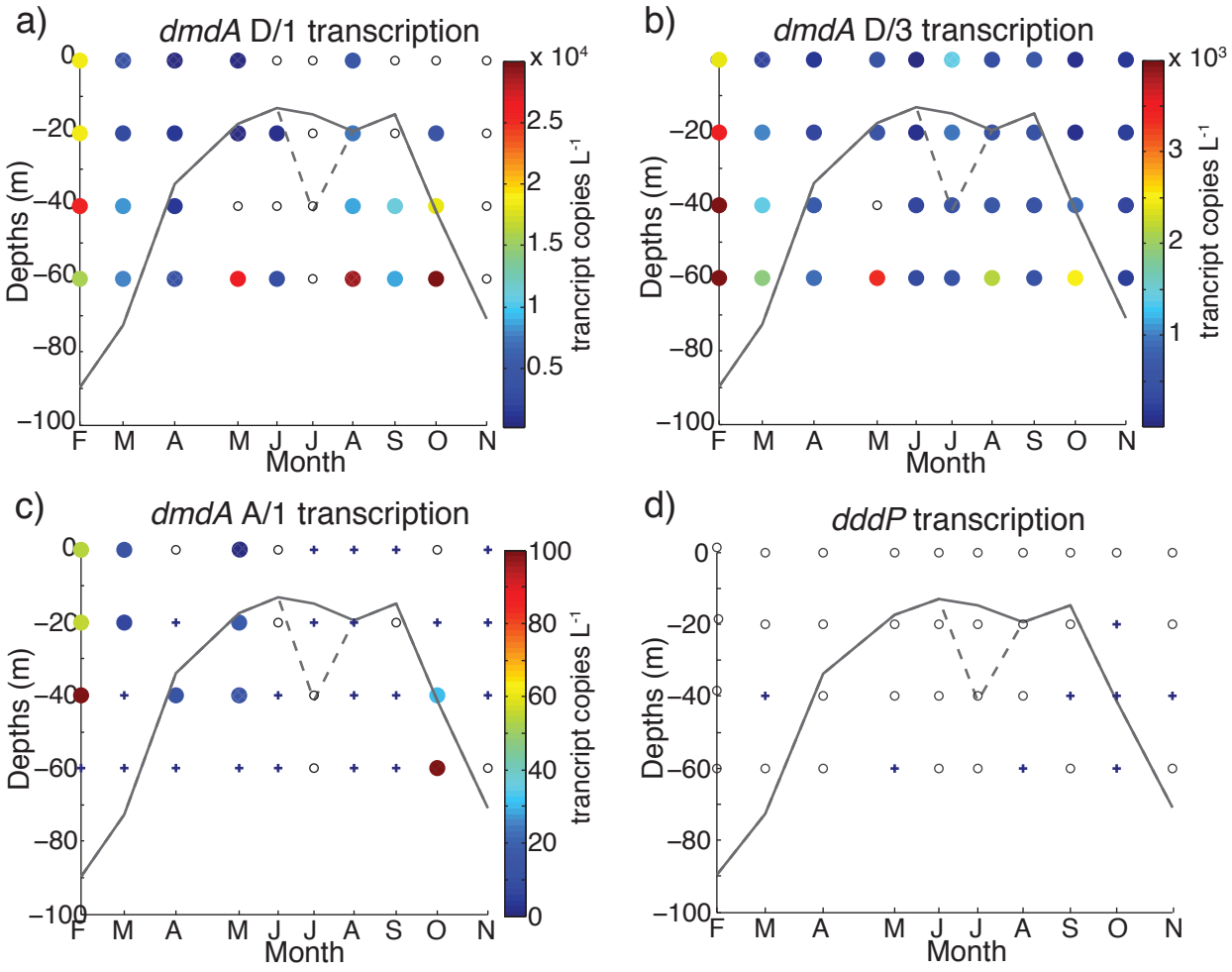
a)
dmdA D/1 transcription
x 10^4
2.5
2
1.5
1
0.5
tranrcipt copies L^-1
Depths (m)
0
−20
−40
−60
−80
−100
F M A M J J A S O N
Month
b)
dmdA D/3 transcription
x 10^3
3
2
1
tranrcipt copies L^-1
Depths (m)
F M A M J J A S O N
Month
c)
dmdA A/1 transcription
100
80
60
40
20
0
tranrcipt copies L^-1
Depths (m)
F M A M J J A S O N
Month
d)
dddP transcription
Depths (m)
F M A M J J A S O N
Month

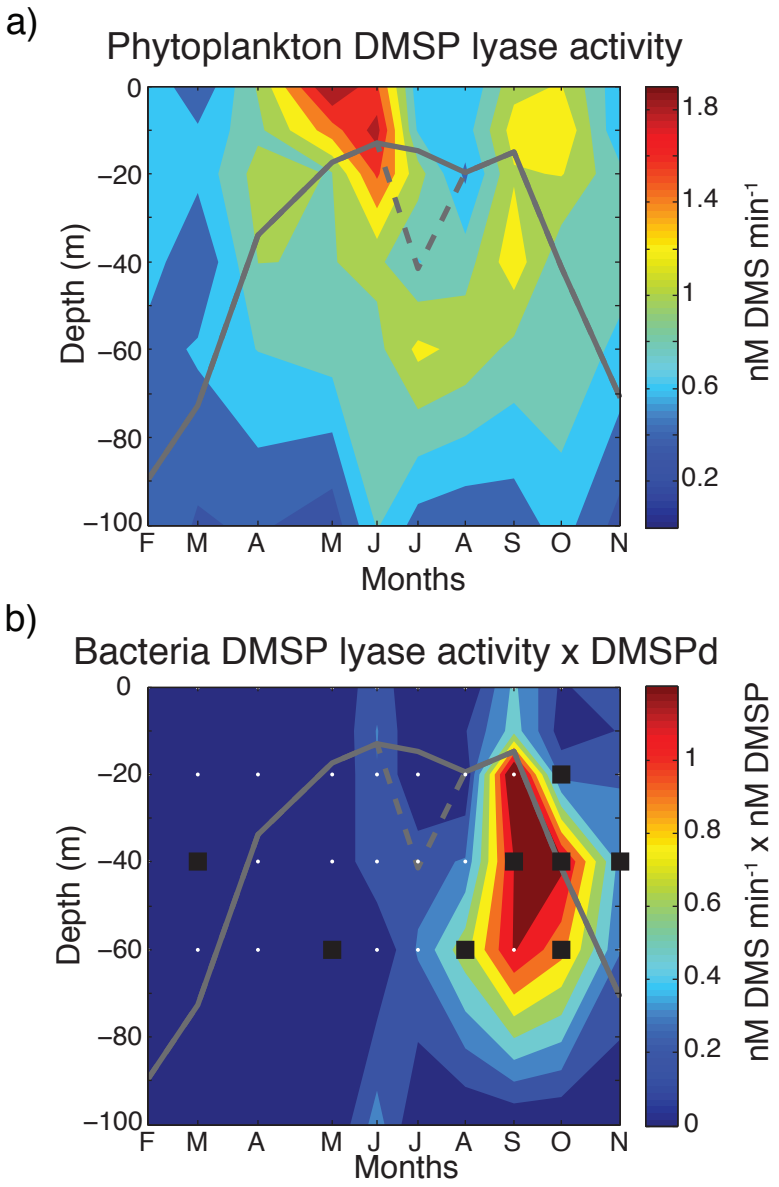
a)
Phytoplankton DMSP lyase activity
Depth (m)
0
−20
−40
−60
−80
−100
F M A M J J A S O N
Months
1.8
1.4
1
0.6
0.2
nM DMS min-1
b)
Bacteria DMSP lyase activity x DMSPd
Depth (m)
0
−20
−40
−60
−80
−100
F M A M J J A S O N
Months
1
0.8
0.6
0.4
0.2
0
nM DMS min-1 x nM DMSP

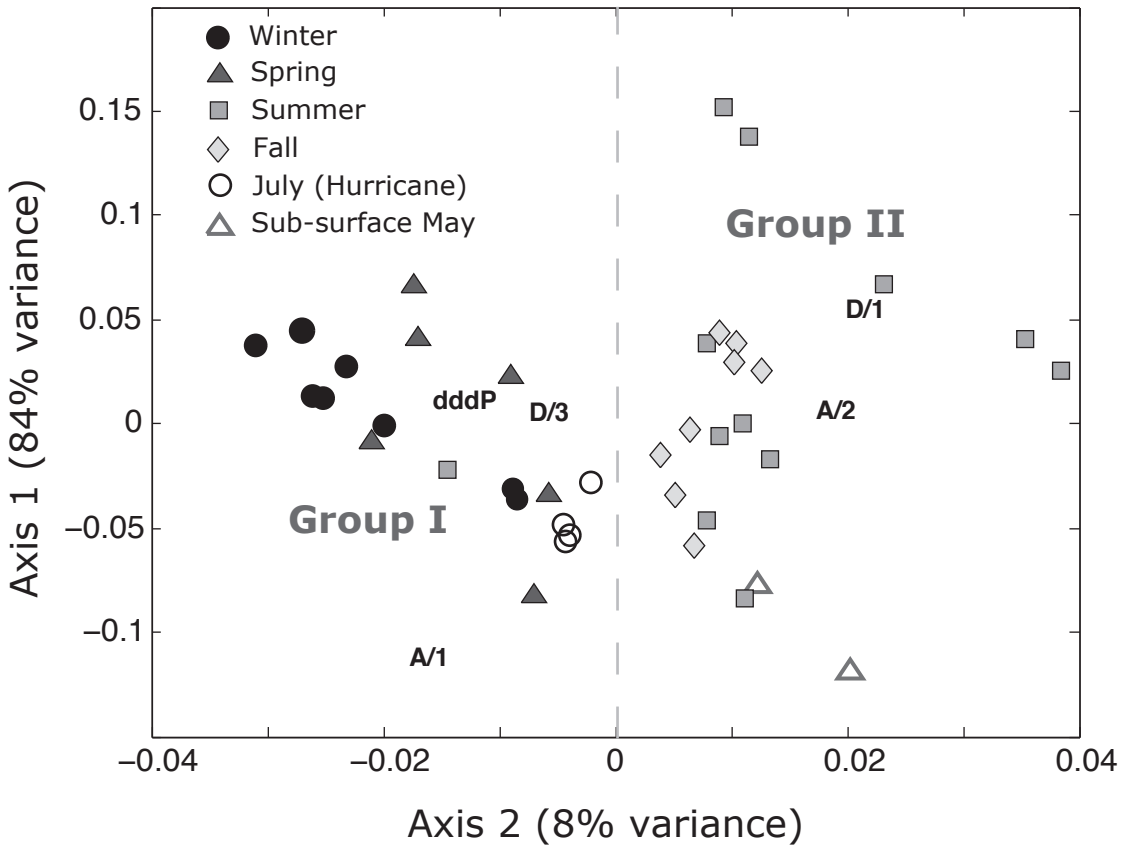
Winter
Spring
Summer
Fall
July (Hurricane)
Sub-surface May
Group I
Group II
dddP
D/3
D/1
A/2
A/1
0.15
0.1
0.05
0
−0.05
−0.1
−0.04
−0.02
0
0.02
0.04
Axis 1 (84% variance)
Axis 2 (8% variance)

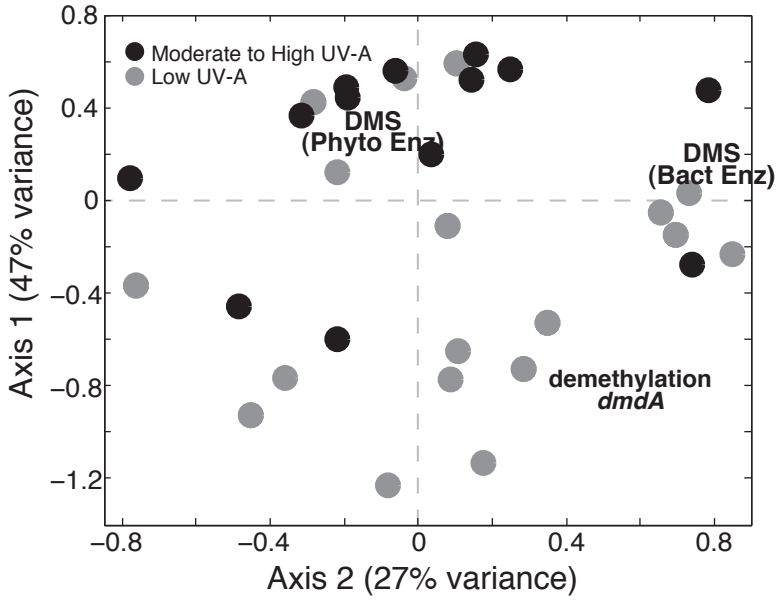
Moderate to High UV-A
Low UV-A
DMS
(Phyto Enz)
DMS
(Bact Enz)
demethylation
dmdA
0.8
0.4
0
−0.4
−0.8
−1.2
−0.8
−0.4
0
0.4
0.8
Axis 1 (47% variance)
Axis 2 (27% variance)

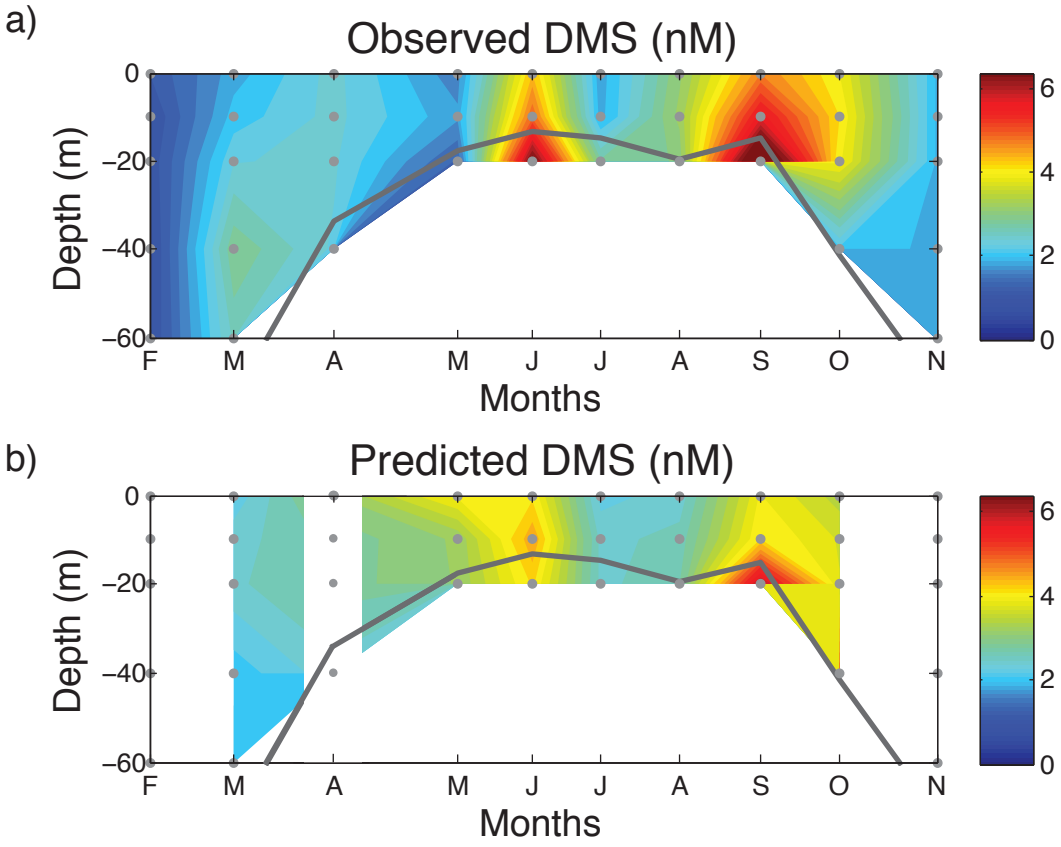
a)
Observed DMS (nM)
Depth (m)
0
−20
−40
−60
F
M
A
M
J
J
A
S
O
N
Months
6
4
2
0
b)
Predicted DMS (nM)
Depth (m)
0
−20
−40
−60
F
M
A
M
J
J
A
S
O
N
Months
6
4
2
0